Modeling of Asymmetric Supercapacitor Cells Based on Electrode's Laboratorial Tests Data

Leonardo Malburg[1(✉)] and Rita Pereira[1,2,3(✉)]

[1] Instituto Superior de Engenharia de Lisboa (ISEL),
R. Conselheiro Emídio Navarro 1, 1959-007 Lisbon, Portugal
a44351@alunos.isel.pt, rpereira@deea.isel.ipl.pt
[2] LCEC, R. Conselheiro Emídio Navarro 1, 1959-007 Lisbon, Portugal
[3] ISRC, Rua Dr. António Bernardino de Almeida, 431, 4200-072 Porto, Portugal

Abstract. This paper concerns the modeling of asymmetric supercapacitor cells based on electrode's data obtained throughout laboratorial tests, such as hydrogen bubble evolution electrodeposition. The electrode's data type here implemented concerns three electrodes system tests, which are designed to provide a single electrode output. This procedure provides instructions on the extraction of electrodes tests parameters, the device's design throughout dimensional basis and comparison with commercially available products and the estimation of energetic output by forecasting the resulting capacitance, voltage, energy and mass of the theoretical supercapacitor.

Keywords: Supercapacitor · Energy storage systems · Hybrid supercapacitor

1 Introduction

Among the various known commercial energy storage devices, supercapacitors or electrochemical capacitors, are highly rated due to their interesting characteristics such as grater power density, cyclability and longer service life [1, 2], resulting in an overwhelming candidate as part of the global energy crisis solution. Such devices can be generically divided in four different types, high voltage ceramic capacitors, electric double-layer capacitors, pseudocapacitors and hybrid supercapacitors [1].

Although the mentioned characteristics, those devices lack energy density when compared to electrochemical batteries, which is fundamental when choosing a long-term device as main energy storage system for a specific implementation [1, 3]. Therefore, promising materials, as is the case of electrodes, have been constantly investigated with higher hopes of surpassing the abovementioned limitation. However, it is not always possible for experimental supercapacitor cells to be produced, which can cause unwanted research setbacks or obstacles. Therefore, this document is focused on modeling of asymmetric supercapacitors of hybrid nature, composed of two different electrode materials of both capacitive and faradaic characteristics, allowing theoretical devices based on experimental electrode materials to be analyzed and implemented in energy storage systems designs, calculations and computational

The original version of this chapter was revised: The numbers in Table 1 and subsequent errors were corrected. The correction to this chapter is available at https://doi.org/10.1007/978-3-030-45124-0_45

L. M. Camarinha-Matos et al. (Eds.): DoCEIS 2020, IFIP AICT 577, pp. 290–298, 2020.
https://doi.org/10.1007/978-3-030-45124-0_27

simulations. Furthermore, this manuscript presents the modeling procedure and calculations of an asymmetric hybrid supercapacitor cell for widespread implementation, accounting for variances in equations regarding the laboratorial data towards cell values.

2 Supercapacitors for Life Improvement

Supercapacitors as a mean of energy storage are a key factor for more efficient and reliable electrical systems [1]. SC's applications encompass mobile and stationary implementations, from transportation to industrial and renewable energy requirements [4]. Macro and micro-scale applications of supercapacitors can be found in the power grid, providing support to power quality improvement that are mainly derived from the growing penetration of renewable generated power into the power grid [5]. Due to distributed generation increasing, the renewable generation can be commonly placed near consumers or even being an integrant part of consumer's electric installations. Considering this power grid point of view, the life improvement is associated with debottlenecking of transmission lines, more reliable integration of renewable energies and consequent greenhouse gas emissions reduction. Moreover, the high-power capabilities can also be addressed to mobile applications regarding power electronics as in electric vehicles (EV) [4], where it performs as a coadjutant device working in parallel with vehicle's battery energy storage system. Supercapacitors not only are able to provide extra power in EV's demand peak situations, but also contributing for an autonomy extension and batteries lifespan increasing throughout the battery cycle's reduction. The methodology addressed in following sections show the theoretical development of a generic hybrid supercapacitor based on an increased performance electrode material that results in better parameters, such as higher capacitance, energy and power density, when compared to a commercial device.

3 Hybrid Supercapacitor Modeling

This paper presents a hybrid supercapacitor (HSC) modeling procedure based on cyclic voltammetry (CV) and galvanostatic charge and discharge curves (GCD) data obtained for both positive and negative electrodes materials [6, 7]. The approach takes into consideration the specific capacitance (C_{sp}), potential window (ΔV), equivalent series resistance (ESR) and reminiscent relevant data, which were gathered from already published laboratorial experiments [6, 7], assumed as primary database for the procedure development. In addition, in order to obtain the theoretical HSC physical structure, a Maxwell 2.3 V 300 F [8] pseudocapacitor was selected as device's choice of design and dimensioning intent, which original size and mass have fit the intended purpose. Therefore, the data set acquired was implemented into the developed electrode-to-cell capacitance equations, from which the individual electrodes capacitances were obtained, thus developing a correlation between electrode and cell data so it could be properly converted.

3.1 From Electrodes to Cell Data

In order to transpose laboratorial data into approximate real values so a device can be modeled and simulated, a correct interpretation of basic equations is required [9]. Based on the general cell capacitance and specific capacitance Eqs. (3.1–3.2) the electrode-to-cell calculation procedure was developed.

$$C_{cell} = \frac{i\Delta t}{\Delta V}[F]. \tag{3.1}$$

$$C_{sp,cell} = \frac{I\Delta t}{m_{total}\Delta V}\left[\frac{F}{g}\right]. \tag{3.2}$$

Where m states for the mass of active material, which correlation for asymmetric cells is defined as in (3.3), I is the current, Δt the time and ΔV the voltage.

$$m_{total} = m_+ + m_-[g]. \tag{3.3}$$

In order to define the specific capacitances equations for asymmetric configurations, firstly, the correlation between cell and both electrodes capacitances must be defined. As described in [9], such correlation can be defined as a series equivalent circuit (3.4), consisting of two electrode-electrolyte interfaces represented as single capacitors C^+ and C^- for the positive and negative electrodes, respectively [10, 11].

$$\frac{1}{C_{cell}} = \frac{1}{C_+} + \frac{1}{C_-}\left[\frac{1}{F}\right]. \tag{3.4}$$

With regards to an asymmetric hybrid supercapacitor configuration, the electrode to cell capacitance is defined by the electrode with smaller capacitance (if $C1 >> C2$, $C_{cell} \approx C2$) [12]. Therefore, as the grater capacitance is not predefined as either positive or negative, $C1$ and $C2$ are hereafter defined as ${C_{elec}}^{c>}$ and ${C_{elec}}^{c<}$, respectively. Consequently, C_{cell} is defined as (3.5).

$$C_{cell} = {C_{elec}}^{c<}[F]. \tag{3.5}$$

Therefore, with regards to asymmetric cells, the specific capacitance can be obtained from (3.6), taking into consideration the total mass (m_{total}) of both active materials.

$$C_{sp,asymm.cell} = \frac{C_{cell}}{m_{total}} = \frac{C_{cell}}{m_+ + m_-} = \frac{{C_{elec}}^{c<}}{m_+ + m_-}\left[\frac{F}{g}\right]. \tag{3.6}$$

Based on (3.5) and (3.6) it is possible to correlate the cell's specific capacitance to the specific capacitance of $C^{c<}$ by considering the cell's total mass as a sum of $m^{c>}$ and $m^{c<}$, defined by (3.7).

$$\frac{C_{cell}}{m_{total}} = \frac{{C_{elec}}^{c<}}{m^{c>} + m^{c<}} = \frac{{C_{elec}}^{c<}}{m^{c<}} = \frac{C_{cell}}{m^{c<}} = {C_{sp.elec}}^{c<}\left[\frac{F}{g}\right]. \tag{3.7}$$

From the equations above it is possible to stablish a relation between two (C_{cell}) and three-electrodes (C_{elec}) results for specific capacitance.

3.2 Electrodes Data

The nickel-copper (Ni-Cu) metallic foam developed in [6] was selected as positive electrode material for the developed HSC, whereas for negative electrode, activated carbon (AC) [7] was implemented. The data were extracted from CVs and GCDs results, as well as scanning electron microscopy (SEM) (as shown in Fig. 1) regarding Ni-Cu electrode-to-electrolyte porosity estimation (the representation shown Fig. 2). The Ni-Cu electrode laboratorial tests [6] have presented a specific capacitance of 105 Fg^{-1} for a material deposition time of 180 s at 1.8 Acm^{-2}. From the CV results [6] a potential window of approximately 1.48 V (−0.5 V to 0.975 V) was obtained for a scan rate of 100 mV s^{-1}. With regards to the AC negative electrode, the considered specific capacitance was of 70 Fg^{-1} [7], even though [26] has presented higher laboratorial results, while a negative potential of −1.0 V with a scan rate of 100 mVs^{-1} [7, 30] was accounted.

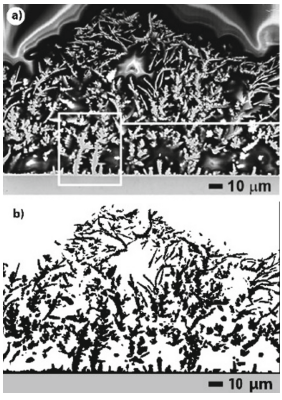

Fig. 1. (a) SEM 1.8 $A.cm^{-2}$ 180 s, electrode section, (b) image enhancing and cleanup [1].

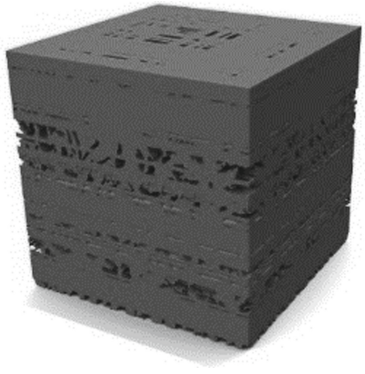

Fig. 2. Electrolyte volume from electrode porosity modelling.

Based on the SEM result addressed in Fig. 1, an enhanced electrode image was obtained via various graphic software from Adobe Creative Suite 6. From the generated image, a generic section of 100 µm was extracted and 3D modeled with the aid of the modeling software Rhinoceros 5.0 [13], which resulted in a sample of 100.10^4 μm^3 representing a proposed Ni-Cu electrode foam structure, from which the total electrode-to-electrolyte volume was obtained (and shown in Fig. 2). From the 3D model a porosity of over 89% was noticed. Despite the difference of foams manufacturing process, when comparing the obtained result with the information gathered from [14],

which stated the material's porosity in the range of 75 to 95%, and based on the statement of [6] that metallic foams porosity values are above 50%, it has considered that the obtained value is acceptable. Therefore, by assuming the porosity values from the manufacturer, 95%, it was possible to calculate the respective electrolyte and electrode volumes shown in Sect. 3.4, Table 1.

3.3 Generic Supercapacitor Dimensioning

The hybrid supercapacitor dimensions were based on a Maxwell 2.3 V 300 F [8] pseudocapacitor. With this purpose, a three-dimensional generic model of such device was developed determining commonly implemented thickness for each of its composing layers as well as the device's general structure. In order to individually identify the volumetric proportion of each part of the base commercial device, a layer stack configuration was assumed based on [15–17].

For the volume distribution supercapacitors, commonly implemented materials were applied. With regards to the device structure it was separated in the following parts: metallic case, terminals, rubber seal, electrodes, current collectors, electrolyte and separator.

As device's metallic case material, an aluminum alloy described as Aluminum 1070, with density of 2.70 gcm^{-3} and thickness of 100 μm, was assumed based on [18, 19]. Regarding the device's terminal, its material was assumed as brass (CuZn37), with density of 8.44 gcm^{-3}, based on [20]. With respect to the rubber seal, the assumed material for its composition was an Ethylene Propylene Diene Monomer (EPDM), with density of 1.40 gcm^{-3} [21, 22]. With regards to the PC electrodes proposed, manganese dioxide (MnO_2) was assumed with a thickness of 0.5 μm and density of 5.02 gcm^{-3} [23–25]. As current collectors an aluminum foil of 2.70 gcm^{-3} density [26] was assumed, which thickness was defined as 30 μm [17]. With regards to the device's electrolyte, potassium hydroxide (KOH) was assumed as it is commonly implemented as such, which density was stated at 1.58 gcm^{-3} [27]. Lastly, the separator material implemented for the developed HSC was the Celgard 2400 [28, 29], defined as a monolayer polypropylene, with thickness of 25 μm and density stated as 0.9 gcm^{-3}. Therefore, based on the presented procedure a generic pseudocapacitor configuration was defined, which resulted in a volume and mass individual distribution regarding each composing part. Furthermore, the generic device corresponded to the original mass stated in the datasheet [8], 24 g, accounting for a total occupied volume of about 7204 mm^3.

3.4 Ni-Cu//AC Hybrid Supercapacitor

Based on the acquired data presented in Sect. 3.2, the Ni-Cu//AC hybrid supercapacitor was developed by replacing the electrodes materials from the generic pseudocapacitor to Ni-Cu and AC parameters, where the total volume was divided equally between positive and negative electrodes.

With regards to the developed hybrid supercapacitor, the intent was to match its final mass to the base Maxwell device. Therefore, with the new materials

implementation the total mass of 24 g was obtained by optimizing the internal case volume filling by its layers stacking, which resulted in a total volume of 14673.8 mm^3 (Table 1).

Therefore, the positive electrode capacitance (C_{elec+}) was obtained by (3.8).

$$C_{elec+} = C_{sp.elec+} m_{elec+} = 105 \times 6.36 \approx 668\,[F]. \tag{3.8}$$

While the AC negative electrode, its capacitance is calculated by (3.9).

$$C_{elec-} = C_{sp.elec-} m_{elec-} = 70 \times 5.71 \approx 400\,[F]. \tag{3.9}$$

Table 1. Ni-Cu//AC hybrid supercapacitor mass redistribution.

Item	Volume (mm^3)	Mass (g)
Metallic case	439.40	1.20
Terminals	49.80	0.42
Rubber seal	1421.00	2.00
AC.Electrode	960.09	0.63
KOH.Electrolyte	3214.19	5.08
Current collector (Al)	2408.24	6.50
Ni-Cu.Electrode	208.71	0.09
KOH.Electrolyte	3965.57	6.27
Separator	2006.79	1.81
Total	14673.8	24.00

Therefore, the cell capacitance (C_{cell}) was defined by assuming the smaller capacitance value ($C_{elec}{}^{c<}$) between both electrodes as described in Sect. 3.1 [12] (3.10).

$$C_{cell} = C_{elec}{}^{c<} = 400\,[F]. \tag{3.10}$$

With regards to the cell voltage, it was proposed based on CV data from both electrodes materials and on [30, 31]. Therefore, based on the stated in [31] that the maximum charging voltage (MCV) for electrodes of different capacitances is obtained by the difference between the biggest potential value for the positive electrode (0.975 V) [6] and the smallest potential for the negative electrode (−1.0 V) [7, 30], ($MCV = E_{P2} - E_{N1}$), the resulting proposed device's rated voltage (V_R) is 1.975 V ≈ 2 V.

The equivalent series resistance (ESR) was calculated according to [32, 33], which is defined by the voltage drop when the charge is interrupted, therefore, obtaining the discharge profile. In order to estimate the possible ESR value for the cell, both electrodes ESRs were obtained from the *IR* drop (3.11–3.12) via GCD graphic interpretation, aided by Rhinoceros 5.0 [13], therefore, the respective data was extracted for the AC electrode from [7, 34, 36], while for the Ni-Cu foam, from [6, 35] 1.8 Acm^{-2} at

180 s sample. The total ESR was considered as the summation of both electrode's internal resistances (Ri_{AC}, $Ri_{Ni\text{-}Cu}$) (3.13).

$$ESR_{AC} = \frac{V_{drop}}{2\Delta I} = \frac{0.07}{2 * 0.01} = 3.5\,[\Omega]. \tag{3.11}$$

$$ESR_{Ni-Cu} = \frac{V_{drop}}{2\Delta I} = \frac{0.019}{2 * 0.001} = 9.5\,[\Omega]. \tag{3.12}$$

$$ESR_{total} = Ri_{AC} + Ri_{Ni-Cu} = 3.5 + 9.5 = 13\,[\Omega]. \tag{3.13}$$

Therefore, the maximum energy storage (3.14) based on [6] and [30], gravimetric specific energy (3.15) [6] were calculated.

$$E_{max.hybrid} = \frac{C.V_R^2 1/2}{3600} \approx 0.23\,[Wh]. \tag{3.14}$$

$$E.sp_{hybrid} = \frac{E_{max.hybrid}}{m} \approx 9.6\left[\frac{Wh}{kg}\right]. \tag{3.15}$$

4 Conclusions

The presented modeling procedure for a theoretical hybrid supercapacitor was developed in order to allow experimental promising electrode materials to be implemented in computational simulations, so their influence and interaction can be analyzed when applied to a wide range of situations, from UPSs to electric vehicle models. With regards to the procedure itself and obtained results, only publication-based analysis and verification where performed, thus experimental confirmation is defined as the next stage of this very study, characterized as future work. Therefore, when analyzing the developed Ni-Cu//AC hybrid supercapacitor results, despite the lack of experimental validation, one can propose that the obtained data has demonstrated promising values when compared to the Maxwell 2.3 V 300 F pseudocapacitor, presenting increased capacitance (400 F), energy (0.23 Wh) and specific energy (9.6 Wh kg^{-1}), which makes it an interesting candidate for further study and development.

References

1. Grbovic, P.J.: Ultra-Capacitors in Power Conversion Systems. Wiley, IEE Press, Chichester (2014). 324 pp.
2. Zhu, C., Lu, R., Tian, L., Wang, Q.: The development of an electric bus with supercapacitors as unique energy storage. In: IEEE Vehicle Power and Propulsion Conference, Windsor, pp. 1–5 (2006)
3. Conway, B.E.: Electrochemical Supercapacitors: Scientific Fundamentals and Technological Applications. Kluwer Academic/Plenum Publishers, New York (1999). 698 pp.

4. Wang, G., Wang, H., Zhong, B., Zhang, L., Zhang, J.: Supercapacitors' Applications. 2016 Taylor & Francis Group, LLC, Electrochemical Energy Storage and Conversion, pp. 479–492 (2015)
5. Fthenakis, V.M., Nikolakakis, T.: Storage options for photovoltaics, Chapt. 11. In: Comprehensive Renewable Energy Encyclopedia, vol. 1, pp. 193–206. Elsevier (2012)
6. Eugénio, S., Silva, T.M., Carmezim, M.J., Duarte, R.G., Montemor, M.F.: Electrodeposition and characterization of nickel-copper metallic foams for application as electrodes for supercapacitors. J. Appl. Elec. **44**(4), 455–465 (2013)
7. Shabeeba, P., Thayyil, M.S., Pillai, M.P., Soufeena, P.P., Niveditha, C.V.: Electrochemical investigation of activated carbon electrode supercapacitors. Russ. J. Elec. **54**(3), 302–308 (2018)
8. Maxwell Technologies: Datasheet: 2.3 V 300F Pseudocapacitor Cell (2018)
9. Roldán, S., Barreda, D., Granada, M., Menéndez, R., Santamaría, R., Blanco, C.: An approach to classification and capacitance expressions in electrochemical capacitors technology. Phys. Chem. **17**, 1084–1092 (2015)
10. Elgrishi, N., Rountree, K.J., McCarthy, B.D., Rountree, E.S., Eisenhart, T.T., Dempsey, J.L.: A practical beginner's guide to cyclic voltammetry. J. Chem. Edu. **95**, 197–206 (2018)
11. Ratha, S., Samantara, A.K.: Supercapacitor: Instrumentation, Measurement and Performance Evaluation Techniques. Springer, Singapore (2018). https://doi.org/10.1007/978-981-13-3086-5
12. Eliaz, N., Gileadi, E.: Physical Electrochemistry: Fundamentals, Techniques, and Applications, vol. 2. Wiley, New York (2019). 480 pp.
13. Rhino 5.0 Product Release. https://www.rhino3d.com/download/Rhino/5.0
14. American Elements – The Materials Science Manufacturer: Datasheet: Ni-Cu Foam (2019)
15. Gualous, H., Louahlia, H., Gallay, R.: Supercapacitor characterization and thermal modelling with reversible and irreversible heat effect. IEEE Trans. Pwr. Elec. **26**, 3402–3409 (2011)
16. Béguin, F., Frackoviak, E.: Supercapacitors: Materials, Systems, and Applications. Wiley-VCH, Weinheim (2013)
17. Obreja, V., Obreja, A.C., Dinescu, A.: Activated carbon based electrodes in commercial supercapacitors and their performance. Int. Rev. Elec. Eng. **5**, 272–282 (2010)
18. Yassine, M., Fabris, D.: Performance of commercially available supercapacitors. Energies **10**, 1340 (2017). 12 pp.
19. Datasheet for Aluminum alloy 1070, manufacturer Indalco: http://www.indalco.com/. Datasheet link: http://www.indalco.com/wp-content/uploads/2013/10/1070.pdf. Accessed 21 Sept 2019
20. Datasheet for Copper alloy CuZn37, manufacturer Arubis: http://www.aurubis-stolberg.com/. Datasheet link: Datasheet CuZn37. Accessed 11 Nov 2019
21. Xu, R., Berduque, A.: Rubber sealing materials for high voltage and high temperature aluminum electrolytic capacitors. In: ECA, pp. 221–236 (2012)
22. Datasheet for Rubber material DRE80 EPDM Rubber, manufacturer Delta: https://shop.deltarubber.co.uk/. Datasheet link: https://shop.deltarubber.co.uk/media/blfa_files/DRE80_EPDM_Rubber_Sheet.pdf. Accessed 21 Sept 2019
23. Girard, H.-L.J.-P.: Modeling and Physical Interpretation of Cyclic Voltammetry for Pseudocapacitors. University of California, Msc. thesis (2015). 97 pp.

24. Safety datasheet for Manganese Dioxide, manufacturer Global Safety management Inc.: https://shop.deltarubber.co.uk/. Datasheet: https://beta-static.fishersci.com/content/dam/fishersci/en_US/documents/programs/education/regulatory-documents/sds/chemicals/chemicals-m/S25420.pdf. Accessed 21 Sept 2019
25. Viswanathan, B.: Fundamentals of chemical conversion processes and applications: Chapter 13 - Supercapacitors. In: Energy Sources, pp. 315–328. Elsevier (2017)
26. Datasheet for ALUMINIUM FOIL EXTRA PURE MSDS, manufacturer Loba Chemie: https://www.lobachemie.com. Datasheet link: https://www.lobachemie.com/lab-chemical-msds/MSDS-ALUMINIUM-FOIL-CASNO-7429-90-00889-EN.aspx. Accessed 21 Sept 2019
27. SAFETY DATA SHEET for Potassium Hydroxide (KOH), manufacturer Merck: https://www.merckgroup.com. Datasheet link: https://www.merckmillipore.com/PT/en/product/msds/MDA_CHEM-109918?ReferrerURL=https%3A%2F%2Fwww.google.com%2F. Accessed 22 Sept 2019
28. Tabatabaei, S.H., Carreau, P.J., Ajji, A.: Microporous membranes obtained from PP/HDPE multilayer films by stretching. J. Membrane Sci. **345**, 148–159 (2009)
29. Datasheet for High Performance Battery Separators, manufacturer Celgard: https://www.celgard.com/. Datasheet link: http://www.jobike.it/Public/data/Daniele%20Consolini/2012517114032_Celgard_Product_Comparison_10002.pdf. Accessed 21 Sept 2019
30. Ye, B., et al.: A high-performance asymmetric supercapacitor based on Ni_3S_2-Coated NiSe arrays as positive electrode. New J. Chem. **43**, 2389–2399 (2018)
31. Dai, Z., Peng, C., Chae, J. H., Chiang, K., Chen, G.Z.: Cell voltage versus electrode potential range in aqueous supercapacitors. Sci. Rep. **5** (2015). 8 pp.
32. Vicentini, R., Silva, L.M., Junior, E.P.C., Alves, T.A., Nunes, W.G., Zanin, H.: How to measure and calculate equivalent series resistance of electric double-layer capacitors. Molecules **24**, 1452 (2019)
33. Keyvan, M., Reza, G.M., Francesca, S.: Toward low-cost and sustainable supercapacitor electrode processing: simultaneous carbon grafting and coating of mixed-valence metal oxides by fast annealing. Front. Chem. **7** (2019). 25 pp.
34. Ahmed, S., Ahmed, A., Rafat, M.: Supercapacitor performance of activated carbon derived from rotten carrot in aqueous, organic and ionic liquid based electrolytes. J. Saudi Chem. Soc. **22**(8), 993–1002 (2018)
35. Mirzaee, M., Dehghanian, C.: Nanostructured Ni-Cu foam electrodeposited on a copper substrate applied as supercapacitor electrode. Acta Metall. Slovaca **24**(4), 325–336 (2018)
36. Liu, R.-S., Zhang, L., Sun, X., Liu, H., Zhang, J.: Electrochemical Technologies for Energy Storage and Conversion, vol. 1. Wiley, New York (2012). 838 pp.